

Effects of Tryptophan Residues of Porcine Myeloid Antibacterial Peptide PMAP-23 on Antibiotic Activity

Joo Hyun Kang, Song Yub Shin, So Yun Jang, Kil Lyong Kim, and Kyung-Soo Hahm¹

Peptide Engineering Research Unit, Korea Research Institute of Bioscience and Biotechnology,
P.O. Box 115, Yusong, Taejeon 305-600, Korea

Received August 30, 1999

PMAP-23 is a 23-residue antimicrobial peptide from porcine myeloid cells. In order to determine the effects of two Trp residues in positions 7 and 21 of PMAP-23 on antibacterial activity and phospholipid vesicle interacting property, two analogues in which Ala is substituted for Trp residue in position 7 or 21 were synthesized. A²¹-PMAP-23 exhibited reduced antibacterial activity and phospholipid vesicle disrupting activity when compared to those of PMAP-23 and A⁷-PMAP-23. PMAP-23 readily interacted with model lipid membrane and induced membrane destabilization. Therefore antibacterial activity induced by PMAP-23 is due to the interaction of cell membrane with peptide followed by membrane perturbation. A significant structural change on the SDS micelle was not found by Ala substitution of the Trp residue of PMAP-23. Also, there is a good correlation between hydrophobic interaction on RP-HPLC, expressed as retention time on RP-HPLC, and antibacterial activity. The vesicle titration experiment indicated that Trp residues located at near C-terminus are accessible to hydrophobic tail of phospholipid vesicle. This result suggests that the C-terminal end of PMAP-23 penetrates into the lipid bilayer in the course of the interaction with phospholipid membranes and is important for its antibacterial activity. © 1999 Academic Press

The antimicrobial peptides have been recognized as an important component of the non-specific host defense system and innate immunity of insects, amphibians, and mammals. The extensively-investigated peptides so far include (a) the inducible antibiotic peptides of insects, (b) the tachyplesin family of peptides found in horseshoe crab species, (c) the antimicrobial peptides secreted by specialized cells in the skin and stomach of amphibia, and (d) the peptides contained in

circulating white cells and mucosal epithelial cells of mammals (1–6).

In mammals, the cytoplasmic granules of neutrophils are an abundant source of a number of antimicrobial peptides, and those identified so far show a significant diversity in structure, spectrum of activity and species distribution (1, 3–6). cDNAs of several neutrophil-derived antibacterial peptides have been cloned based on preproregion homology in the precursors and their cDNA sequences indicate that they are generally synthesized as precursors that release the mature, biologically active peptide after proteolytic cleavage. These include Arg-rich and Pro-rich peptides such as Bac5 and Bac7 (7, 8), PR-39 (9) and C12 (10), α -helical peptides such as CAP18 (11) and PMAP-36 (12), Cys-containing peptides such as the cyclic dodecapeptide (13) and the protegrins (14, 15) and other peptides such as the Trp-rich indolicidin (16).

PMAP-23 peptide was identified by cDNA cloning and shown to possess a potent antimicrobial activity with chemically synthesized peptide (17). PMAP-23 is highly cationic with 5 Arg and 2 Lys residues and has 11 highly hydrophobic residues including 2 Trp. Therefore PMAP-23 is tend to form some amphipathic structure, which is typical of antibacterial peptides.

In this paper, the effects of two Trp residues of PMAP-23 on antibiotic activity and phospholipid vesicle disrupting properties were investigated by analyzing the hydrophobicity and secondary structure of peptides. Also we will discuss which tryptophan residue is important for the phospholipid vesicle interaction.

MATERIALS AND METHODS

Peptide synthesis. The peptides were synthesized by the solid phase method using Fmoc(9-fluorenyl-methoxycarbonyl)-chemistry (18). Arg(pmc)-Wang-Resin was used as the support to obtain a C-terminal free peptide. The coupling of Fmoc-amino acids was performed with N-hydroxybenzotriazole (HOBt) and dicyclohexylcarbodiimide (DCC). Amino acid side chains were protected as follows: *tert*-butyl (Asp and Thr), trityl (Gln), *tert*-butyloxycarbonyl (Lys and Trp), pmc (Arg). Deprotection and cleavage from the resin were

¹ To whom correspondence should be addressed. Fax: + 81 42 860 4593. E-mail: hahmks@kribb4680.kribb.re.kr.

carried out using a mixture of trifluoroacetic acid, phenol, water, thioanisole, 1, 2-ethanedithiol and triisopropylsilane (82.5:5:5:5:2.5:2, v/v) for 3 hr at room temperature. The crude peptide was then repeatedly washed with diethylether, and dried in a vacuum. The crude peptides were purified by a reversed-phase preparative HPLC on a Waters 15- μ m Deltapak C₁₈ column (19 \times 30 cm). The purified peptides were hydrolyzed with 6 N-HCl at 110°C for 22 h, and then dried in a vacuum. The residues were dissolved in 0.02 N HCl and subjected to an amino acid analyzer (Hitachi Model, 8500 A, Japan). Peptide concentration was determined by amino acid analysis. The molecular masses of the peptides were confirmed with MALDI (matrix-assisted laser desorption/ionization) mass spectrometer. Analytical RP-HPLC was carried out using a Ultrasphere C₁₈ column (Beckman, USA), 4.6 \times 25 cm. Samples were monitored at 214 nm on Hitachi L-3000 photodiode array detector. Buffer A consisted of 0.05% TFA in water and buffer B of 0.05% TFA in 80% acetonitrile. The peptides were eluted with a 30 min linear gradient (20–60%) of buffer B.

Antibacterial activity. *Escherichia coli* (KCTC 1682), *Salmonella typhimurium* (KCTC 1926), *Pseudomonas aeruginosa* (KCTC 1637), *Bacillus subtilis* (KCTC 1918), *Streptococcus pyogenes* (KCTC 3096), and *Staphylococcus aureus* (KCTC 1621) were supplied from the Korean Collection for Type Cultures (KCTC), Korea Research Institute of Bioscience & Biotechnology (Taejon, Korea). The bacteria were grown to the mid-logarithmic phase in a LB medium (g/l) [10 bactotryptone/5 yeast extract/10 NaCl (pH 7.0)]. The peptides were filtrated through a 0.22 μ m filter and stepwise-diluted in a medium of 1% bactopectone. The tested organism (final bacterial suspension: 2×10^6 colony formation units (CFU)/ml) suspended in growth medium (100 μ l) was mixed with 100 μ l of the two-fold diluted serial solution of each peptide in a microtiter plate well with three replicates for each test sample. The plates were incubated for 18 hr at 37°C. The minimal inhibitory concentration (MIC) was defined as the lowest concentration of peptide which gave no visible growth on the plate. The kinetics of bacterial killing of the peptides was evaluated using *E. coli* and *B. subtilis*. Log-phase bacteria (6×10^5 CFU/ml) were incubated with 5 μ M peptide in LB. Aliquots were removed at fixed time intervals, appropriately diluted, plated on LB broth agar plate, and then the colony-forming units were counted after 16–18 h incubation at 37°C.

Hemolytic activity. The hemolytic activity of the peptides was evaluated by determining the released hemoglobin of 4% suspensions of fresh human erythrocytes at 414 nm (19, 20). Human red blood cells were centrifuged and washed three times with phosphate-buffered saline (PBS: 35 mM phosphate buffer/0.15 M NaCl, pH 7.0). One hundred μ l of human red blood cells suspended 8% (v/v) in PBS were plated into 96-well plates, and then 100 μ l of the peptide solution was added to each well. The plates were incubated for 1 hr at 37°C, and centrifuged at 150 g for 5 min. One hundred μ l aliquots of the supernatant were transferred to 96-well plates. Hemolysis was measured by absorbance at 414 nm with an ELISA plate reader (Molecular Devices Emax, Sunnyvale, CA, USA). Zero percent and 100% hemolysis were determined in PBS and 0.1% Triton-X 100, respectively. The hemolysis percentage was calculated using the following equation: % hemolysis = [(Abs_{414 nm} in the peptide solution – Abs_{414 nm} in PBS)/(Abs_{414 nm} in 0.1% Triton-X 100 – Abs_{414 nm} in PBS)] \times 100.

Circular dichroism (CD) spectroscopy. CD spectra of peptides were recorded using a Jasco J720 spectropolarimeter using a 1 mm pathlength cell (Tokyo, Japan). The CD spectra of the peptides in 10 mM sodium phosphate buffer (pH 7.2), 50% (v/v) TFE, 30 mM SDS or 30 mM DPC were recorded at 25°C in the 190–240 nm wavelength range at 0.1 nm intervals. The peptide concentrations were 100 μ g/ml. The mean residue ellipticity $[\theta]$ was calculated using the molecular weight of each peptide as determined from the amino acid composition.

TABLE 1

Amino Acid Sequence of PMAP-23 and Its Analogues

Peptides	Sequences
PMAP-23	RIIDLLWRVRRPQKPKEFVTWVR
A'-PMAP-23	RIIDLLARVRRPQKPKEFVTWVR
A ²¹ -PMAP-23	RIIDLLWRVRRPQKPKEFVTVAVR

Note. The bolded amino acids indicate substituted amino acid in PMAP-23.

Phospholipid vesicle preparation. Small unilamellar vesicle (SUV) composed of phosphatidylcholine (PC)/phosphatidylserine (PS) (4:1, wt/wt) or phosphatidylcholine (PC) were prepared by sonication (21) and large unilamellar vesicle (LUV) with PC/PS (4:1) was prepared by reverse-phase ether evaporation method (22), followed by the extrusion through 400 nm polycarbonate filters of Liposofast Extruder (Avestin Inc., Canada). LUV encapsulated with carboxy-fluorescein (CF) was prepared in a solution of 100 mM CF and the unencapsulated CF in the vesicle suspension was removed by gel-filtration on a Bio-Gel A-0.5m (Bio-Rad, CA, USA) column (1.5 \times 30 cm) using 0.15 M NaCl/10 mM sodium phosphate buffer (pH 7.4).

Release of CF from lipid vesicle. Release of CF from phospholipid vesicle was monitored in the presence of peptide at different concentrations. The released CF fluorescence was detected by measuring fluorescence intensity at 520 nm excited at 490 nm on a Shimadzu RF-5000 spectrofluorometer (Tokyo, Japan) under constant stirring. The phospholipid concentration of vesicle suspension used in this study was 6.36 μ M. The apparent percent leakage value at a fluorescence intensity, F, was calculated by the following equation:

$$\% \text{ leakage (apparent)} = 100 \times (F - F_0)/(F_t - F_0)$$

F_t denotes the fluorescence intensity corresponding to 100% leakage after the addition of 20 μ l of 10% Triton X-100. F₀ represents the fluorescence of the intact vesicle.

Determination of vesicle aggregation. Phospholipid vesicle aggregating activity of the peptides was measured by the changes in turbidity at 400 nm using a Beckman DU-8 spectrophotometer (Palo Alto, CA). SUV of PC/PS (4:1) was suspended in 150 mM NaCl/10 mM HEPES (pH 7.4) to give a final concentration of 35 μ M. Various amounts of the peptides were added to the vesicle suspension to obtain various ratios of peptide to phospholipid. The absorbance data were taken after 10 min incubation with peptide.

Fluorescence of tryptophan residue. Tryptophan fluorescence measurements were performed using spectrofluorometer. Appropriate aliquots of PC:PS (4:1) LUV were successively added to a solution of 1.5 ml of peptide in Hepes buffer. After each addition of vesicle, the mixture was kept at 25°C for 10 min to achieve the equilibration. Spectral measurements were recorded at an excitation wavelength of 280 nm and emission wavelength of 300 to 400 nm. The bandwidth of excitation and emission was 5 and 3 nm, respectively. The various amounts of LUV suspension was added to the peptide solutions of 0.67 μ M.

RESULTS

Peptide Design and Antibacterial Activities

All peptide used in this study was summarized in Table 1. The synthetic peptides were purified by the reverse-phase HPLC and quantified by amino acid analysis. The correct molecular weights of the syn-

TABLE 2

Molecular Weight Determined by MALDI-MS and RP-HPLC Retention Times of PMAP-23 and Its Analogues

Peptides	Calculated value	Observed value	Retention time (min)
PMAP-23	2962.6	2963.4	16
A ⁷ -PMAP-23	2847.5	2848.2	15
A ²¹ -PMAP-23	2847.5	2848.1	14.5

thetic peptides were confirmed by MALDI mass spectrometry (Table 2). It is well known that retention time on RP-HPLC can be used as a measure of peptide hydrophobicity (23, 24). Despite their identical composition and same intrinsic hydrophobicity of A⁷-PMAP-23 and A²¹-PMAP-23, these peptides had the differences in the retention time (15 min of A⁷-PMAP-23 and 14.5 min of A²¹-PMAP-23, Table 2). The differences in retention time were attributed to the induced conformational changes upon interaction with the C₁₈ of the RP-HPLC stationary phase.

Antibacterial activities of the peptides for gram-positive and gram-negative bacteria were determined as MIC by the microdilution test (Table 3). PMAP-23 and A⁷-PMAP-23 (Trp⁷ → Ala) showed similar antibacterial activity against both gram-negative bacteria (*E. coli*, *S. typhimurium*, and *P. aeruginosa*) and gram-positive bacteria (*B. subtilis*, *S. pyogenes* and *S. aureus*) at concentrations ranging from 1.56 to 3.125 μM. However, Trp²¹ → Ala (A²¹-PMAP-23) substitution in PMAP-23 resulted in about 2-fold decrease in antibacterial activity. The bactericidal time course of the peptide to logarithmic phase of *E. coli* and *B. subtilis* was determined. As shown in Fig. 1, PMAP-23 displayed faster bactericidal rate against both *E. coli* and *B. subtilis* than A⁷-PMAP-23 and A²¹-PMAP-23. These results indicate that two Trps of PAMP-23 have an important role in bactericidal activities against both *E. coli* and *B. subtilis*. The cytotoxicity of peptides against normal eukaryotic cells was determined by monitoring the released hemoglobin from incubating 4% human red blood cell suspension. None of peptide exhibited any hemolytic activity even at 100 μM (Table 3).

TABLE 3

Antibacterial Activities and Hemolytic Activities of PMAP-23 and Its Analogues

Peptides	MIC: μM						% Hemolysis (100 μM)
	<i>E. coli</i>	<i>S. typhimurium</i>	<i>P. aeruginosa</i>	<i>B. subtilis</i>	<i>S. pyogenes</i>	<i>S. aureus</i>	
PMAP-23	1.56	1.56	1.56	1.56	1.56	3.125	0
A ⁷ -PMAP-23	3.125	1.56	1.56	1.56	1.56	3.125	0
A ²¹ -PMAP-23	6.25	3.125	3.125	3.125	3.125	6.25	0

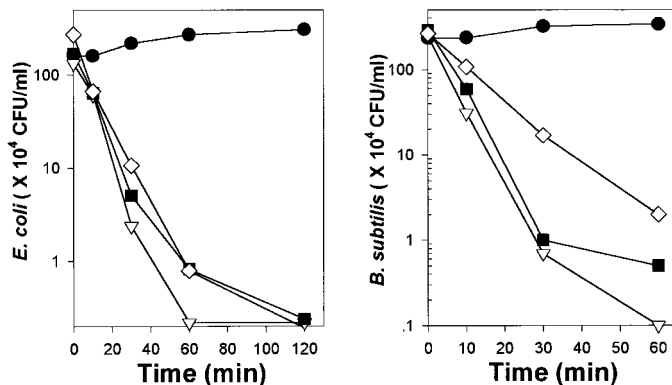


FIG. 1. Time killing plots for *E. coli* and *B. subtilis* by PMAP-23 and its analogues. Bacteria, either untreated (●) or treated with 5 μM of peptide, PMAP-23 (◇), A⁷-PMAP-23 (■), or A²¹-PMAP-23 (△), were diluted at the indicated time intervals, and then plated on LB broth agar. The colony forming units were calculated by counting the colony after 16–18 hr incubation at 37°C.

Structure Analysis

The CD spectra of the peptides were measured in sodium dodecyl sulfate (SDS) solution as lipid membrane-mimicking solvent (Fig. 2). In 10 mM sodium phosphate buffer, PMAP-23 and its analogues showed an unordered structure, which had a strong negative ellipticity at near 200 nm. These peptides exhibited the mixed conformation of some α-helix and β-turn structure judged by a negative ellipticity at near 205 nm (25) in SDS solution. Therefore the conformational changes may not be induced by any Trp → Ala substitution or by position of Trp residue.

Peptide-Induced Phospholipid Vesicle Aggregation and Disruption

In order to investigate the membrane-interacting mechanism of peptides, the vesicle aggregation events were examined as the initial step of peptide-vesicle interaction. The changes in vesicle size due to peptide-induced aggregation were measured as a function of peptide concentration by an absorbance of vesicle suspension at 400 nm. The light scattering intensity is known to be quite sensitive to particle size. Figure 3

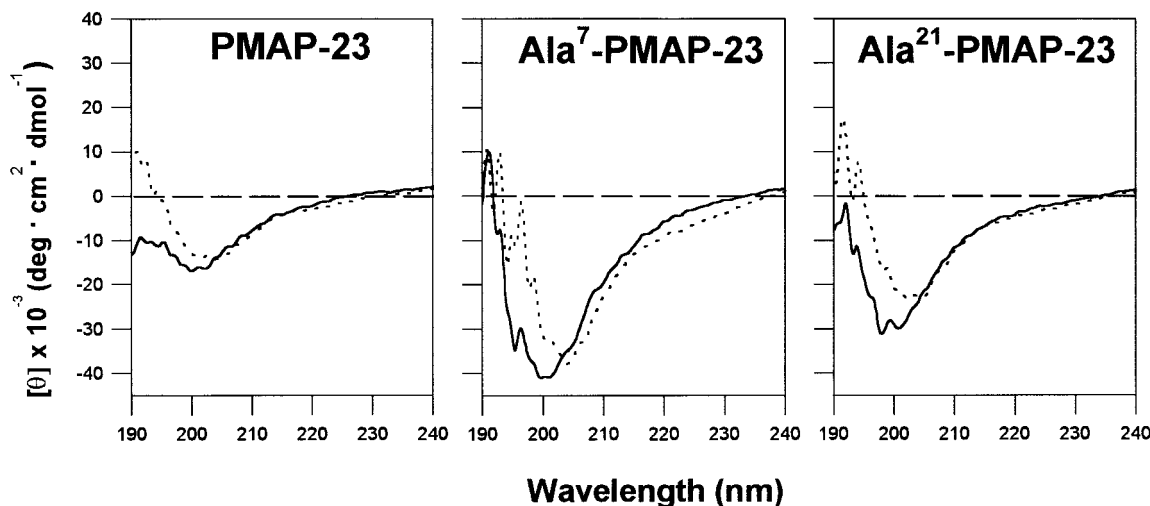


FIG. 2. CD spectra of PMAP-23 and its analogues in the solutions of 30 mM SDS (···), and 10 mM sodium phosphate buffer, pH 7.2 (—).

showed the peptide-induced absorbance increases in PC:PS (4:1) or PC vesicle. When PMAP-23 was added to PC:PS (4:1) vesicle solution, the greater absorbance increase due to effective aggregation was observed than other analogues. Ala-substituted analogues in Trp residues caused a significant reduction in vesicle aggregation and A²¹-PMAP-23 had the lowest vesicle aggregation activity. The efficiency of zwitterionic PC vesicle aggregation (Fig. 3, inset) by peptide was 50–100 fold lower than that of PC:PS (4:1) vesicle containing negatively charged phospholipid. The interaction of the peptides with phospholipid vesicles was further

investigated by measuring the ability of the peptide to perturb the PC:PS (4:1) LUVs (Fig. 4). PMAP-23, which induced the effective vesicle aggregation, exhibited the highest activity in the vesicle disruption. This result suggested that the relative efficiencies of PMAP-23 and its analogues to perturb the lipid membranes were correlated with their vesicle aggregation activities.

Fluorescence of Trp Residue of Peptide with Phospholipid Vesicle

The high sensitivity of Trp fluorescence to the polarity of the environment can provide information about peptide-phospholipid interactions (26). Sinking of Trp residue in the aliphatic portion of the phospholipid bilayer would result in a blue shift of Trp fluorescence emission and a decrease of fluorescence intensity of maximum emission wavelength of peptide in a buffer solution. Fluorescence spectra of PMAP-23 and its analogues in buffer solution showed an emission maxima at near 350 nm. The fluorescence emission spectra of peptides were recorded in the presence or absence of vesicles. The fluorescence intensity of PMAP-23 and A⁷-PMAP-23 at 350 nm decreased with the addition of vesicle suspension and reached to a saturated level at same phospholipid amount. However, the fluorescence pattern of A²¹-PMAP-23 by vesicle was different from that of PMAP-23. The interaction pattern of A⁷-PMAP-23 with vesicle was similar to that of PMAP-23 and Trp at position 21 might be important for the peptide-vesicle interaction.

DISCUSSION

PMAP-23 showed strong antibacterial activity against Gram-positive and negative strains but did not

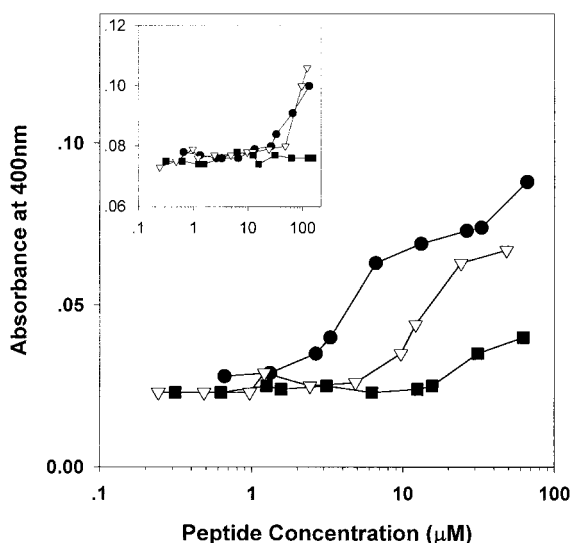


FIG. 3. Monitoring the phospholipid vesicle (PC/PS, 4:1) aggregation induced by peptides. The vesicle aggregation was determined by measuring the absorbance at 400 nm. ●, PMAP-23; ▽, A⁷-PMAP-23; ■, A²¹-PMAP-23. (Inset) The aggregation efficiency of phospholipid vesicle containing PC lipid by peptides.

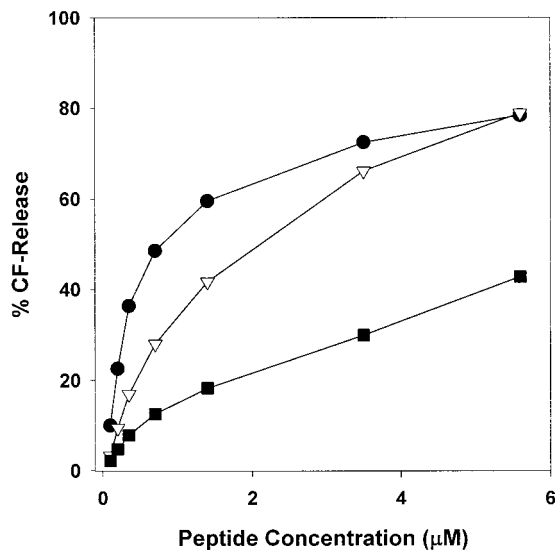


FIG. 4. Release of CF from LUVs composed of PC:PS (4:1). The extents of vesicle disruption induced by peptide were indicated as a function of peptide concentration. The released CF fluorescence was measured at $\lambda_{\text{ex}} = 490$ nm and $\lambda_{\text{em}} = 520$ nm. ●, PMAP-23; ▽, A⁷-PMAP-23; ■, A²¹-PMAP-23.

exhibit lytic activity against human erythrocytes at a concentration of upto 100 μM , suggesting it has certain degree of target cell membrane specificity. Trp residue in antibacterial peptides including cecropin A is known to be important for the antibacterial activity (27). Therefore, the effect of two Trp residues at position 7 and 21 of PMAP-23 on antibacterial activities was investigated by Trp⁷ \rightarrow Ala or Trp²¹ \rightarrow Ala substitutions. A²¹-PMAP-23 exhibited weaker antibacterial activity than PMAP-23 and A⁷-PMAP-23. Therefore Trp residue at position 21 appears to play an important role in an antibacterial activity. However, the secondary structure of these peptides in SDS micelle might not be necessary for the antibacterial activity since Trp \rightarrow Ala substitutions of peptide did not result in the structural changes. RP-HPLC has been found to have significant potential for studying the hydrophobicity of peptide induced at aqueous/lipid interfaces. Separation of peptides during RP-HPLC is known to be primarily due to the different hydrophobic interactions of the individual peptides with the lipid groups of the stationary phase. Such interactions can be considered to be comparable to the hydrophobic interactions during biological processes. For example, a series of peptide analogues of melittin exhibited the correlation between retention time and hemolytic activities (28). Although A⁷-PMAP-23 and A²¹-PMAP-23 had same intrinsic hydrophobicity, A⁷-PMAP-23 had a slightly longer retention time and higher antibacterial activity than A²¹-PMAP-23. Therefore there is a good correlation between hydrophobic interaction on RP-HPLC and antibacterial activity.

Furthermore, to determine the action mechanisms of these peptides on antibacterial activity, we studied the interaction of PMAP-23 and its two analogues with phospholipid vesicle. PMAP-23 and its analogues aggregated effectively PC/PS (4:1) vesicle compared to zwitterionic PC vesicle. This result suggests that the electrostatic interaction of cationic peptide PMAP-23 with negatively charged phospholipid vesicle is necessary for the peptide-vesicle interaction event. Although the basicity of A²¹-PMAP-23 was identical to that of A⁷-PMAP-23, A²¹-PMAP-23 rarely induced the vesicle aggregation. This result indicates that in order to induce the peptide-vesicle interaction, another factors were needed, i.e. hydrophobic interaction of peptide-lipid vesicles, in addition to electrostatic interaction. PMAP-23 readily interacted with artificial lipid membrane, rapidly aggregated and induced membrane destabilization, as manifested by the leakage of vesicle contents. In an attempt to determine the accessible Trp residue of position 7 or 21 to lipid bilayer, the spectroscopic titration of peptide was performed with the addition of phospholipid vesicle suspensions (Fig. 5). PMAP-23 and A⁷-PMAP-23 with Trp residue in position 21, showed similar fluorescence titration pattern compared to A²¹-PMAP-23. Therefore Trp residue located at near C-terminus (position 21) was accessible to hydrophobic tail of phospholipid vesicle and was important for the antibacterial activity and the interaction with phospholipid vesicle. The relative efficiency of the peptides to perturb the lipid membranes correlated to their an-

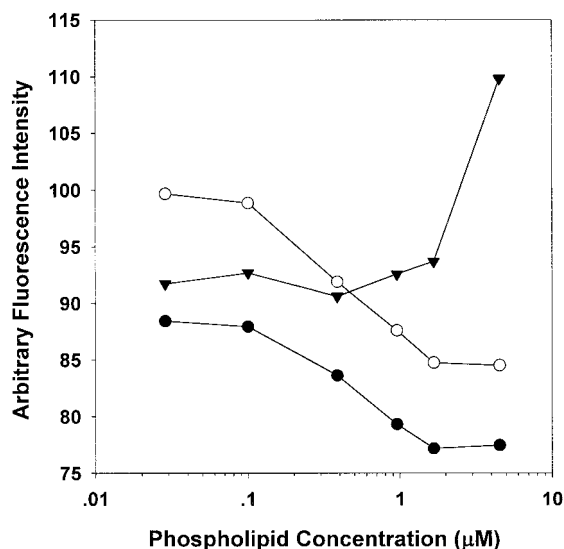


FIG. 5. Phospholipid titration curves induced by peptides. The indicated amount of PC:PS (4:1) LUV was successively added to the peptide solution. The spectral measurements were recorded by the fluorescence intensity at emission wavelength of 350 nm, excited at 280 nm. ●, PMAP-23; ○, A⁷-PMAP-23; ▼, A²¹-PMAP-23.

tibacterial activity. This result suggests that the antibacterial activity induced by PMAP-23 is due to the interaction of cell membrane with peptide, followed by membrane perturbation.

In conclusion, Trp residue in position 21 of PMAP-23 affected on the antibacterial activity and phospholipid vesicle disrupting activity as well as the hydrophobicity on RP-HPLC. Therefore, the C-terminal end of PMAP-23 maybe penetrate primarily into the lipid bilayer in the course of phospholipid membrane interaction of PMAP-23.

REFERENCES

1. Boman, H. G (1991) *Cell* **65**, 205–207.
2. Hoffman, J. A., and Hetru, C. (1992) *Immunol. Today* **13**, 411–415.
3. Zasloff, M. (1992) *Curr. Opin. Immunol.* **4**, 3–7.
4. Gennaro, R., Romeo, D., Skerlavaj, B., and Zanetti, M (1991) in *Blood Cell Biochemistry* (Harris, J. R., Ed.), Vol 3, pp. 335–368, Plenum, New York.
5. Weiss, J. (1994) *Curr Opin Hematol* **1**, 78–84.
6. Lehrer, R. I., Lichtenstein, A. K., and Ganz, T. (1993) *Annu. Rev. Immunol.* **11**, 105–128.
7. Zanetti, M, Del Sal, G., Storici, P., Schneider, C., and Romeo, D. (1993) *J. Biol. Chem.* **268**, 522–526
8. Scocchi, M., Romeo, D., and Zanetti, M. (1994) *FEBS Lett* **352**, 197–200.
9. Storici, P., and Zanetti, M (1993) *Biochem. Biophys. Res. Commun.* **196**, 1058–1065.
10. Pungercar, J., Strukelj, B., Kopitar, G., Renko, M., Lenarcic, B., Gubensek, F., and Turk, V. (1983) *FEBS Lett*, **336**, 284–288.
11. Larrick, J. W., Morgan, J. G., Palings, I., Hirata, M., and Yen, M. H. (1991) *Biochem. Biophys. Res. Commun.* **179**, 170–175.
12. Storici, P., Scocchi, M., Tossi, A., Gennaro, R., and Zanetti, M. (1994) *FEBS Lett.* **337**, 303–307.
13. Storici, P., Del Sal, G., Schneider, C., and Zanetti, M. (1992) *FEBS Lett* **314**, 187–190.
14. Storici, P., and Zanetti, M (1993) *Biochem. Biophys. Res. Commun.* **196**, 1363–1368.
15. Zhao, C., Liu, L., and Lehrer, R. I. (1994) *FEBS Lett.* **346**, 285–288.
16. Del Sal, G., Storici, P., Schneider, C., Romeo, D., and Zanetti, M. (1992) *Biochem. Biophys. Res. Commun.* **187**, 467–472.
17. Zanetti, M., Storici, P., Tossi, A., Scocchi, and Gennaro, R. (1994) *J Biol. Chem.* **269**, 7855–7858.
18. Merrifield, R. B. (1986) *Science* **232**, 341–347.
19. Andreu, D., Ubach, J., Boman, A., Wahlin, D., Wade, D., Merrifield, R. B., and Boman, G. (1992) *FEBS Lett.* **296**, 190–194.
20. Shin, S. Y., Kang, J. H., and Hahm, K.-S. (1999) *J. Peptide Res.* **53**, 82–90.
21. Ohki, S. (1982) *Biochim. Biophys. Acta* **689** 1–11.
22. Duzgunes, N., Wilschut, J., Hong, K., Fraley, R., Perry, C., Friend, D., James, T. L., and Paphadjopoulos, P. (1983) *Biochim. Biophys. Acta.* **732**, 289–299.
23. Parker, J. M. R., Guo, D., and Hodges, R. S (1986) *Biochemistry* **25**, 5425–5432.
24. Guo, D., Mant, C. T., Taneja, A. K., Parker, J. M. R., and Hodges, R. S. (1986) *J. Chromatogr.* **359**, 499–517.
25. Perczel, A., and Hollosi, M (1996) *Circular Dichroism and the Conformational Analysis of Biomolecules* (Fasman, G. D., Ed.), pp. 285–380, Plenum Press, New York.
26. Ladokhim, A. S., Selsted, M. E., and White, S. H. (1997) *Biophys. J.* **72**, 794–804.
27. Andreu, D., Merrifield, R. B., Steiner, H., and Boman, H. G. (1983) *Proc. Natl. Acad. Sci USA* **80**, 6475–6479.
28. Blondelle, S. E., and Houghten, R. A. (1991) *Biochemistry* **30**, 4671.